^{1}H NMR study of proton dynamics in the inorganic solid acid Rb$_3$H(SO$_4$)$_2$

Koh-ichi Suzuki and Shigenobu Hayashi*

Research Institute of Instrumentation Frontier, National Institute of Advanced Industrial Science and Technology (AIST),
Tsukuba Central 5, 1-1-1 Higashi, Tsukuba, Ibaraki 305-8565, Japan

Proton dynamics in Rb$_3$H(SO$_4$)$_2$ has been studied by means of ^{1}H NMR. The ^{1}H magic-angle-spinning (MAS) NMR spectra were traced at room temperature (RT) at Larmor frequency of 400.13 MHz. ^{1}H static NMR spectra were measured at frequencies of 200.13 MHz and 400.13 MHz in the ranges of 165–513 and 300–513 K, respectively. ^{1}H spin-lattice relaxation times, T_1, were measured at 200.13 and 19.65 MHz in the ranges of 260–513 and 260–470 K, respectively. The ^{1}H MAS NMR spectrum at 294 K has an isotropic chemical shift of 16.3 ppm from tetramethylsilane, demonstrating very strong hydrogen bonds. In RT phase, a wobbling motion of the O-H axis in one direction at the fast motional limit takes place above 400 K, being supported by the ^{1}H static NMR spectral line shapes and by the ^{1}H T_1 values. In the high temperature (HT) phase, the sharp ^{1}H static NMR spectra indicate translational proton diffusion. From the analysis of ^{1}H T_1, protons diffuse with the inverse of the frequency factor (τ_0) of 9.5×10^{-13} s and the activation energy (E_a) of 25 kJ mol^{-1}. These parameters can well explain the macroscopic electric conductivity in HT phase.

I. INTRODUCTION

Fuel cells are attractive for electrical power generation because of their high efficiencies and low pollution levels. The electrolyte membranes are indispensable to the fuel cells. As polymer electrolyte membranes require humid atmospheres, the operating temperature range is limited to lower than 100 °C. Haile *et al.*[1,2] pointed out the advantage of solid acids as fuel cell electrolytes due to circumvent the above limits. They demonstrated that water-soluble inorganic solid acids such as CsHSO$_4$ are used successfully in H$_2$/O$_2$ fuel cells, although several improvements are necessary before their practical use.

It is well known that a high proton conductivity is observed in a high-temperature phase, so-called "a superprotonic phase," of solid acids such as MHXO$_4$ and M_3H(XO$_4$)$_2$ (M=Cs, NH$_4$, Rb; X=S, Se) families.[3–6] Previously, we reported the proton dynamics in CsHSO$_4$ and Cs$_2$(HSO$_4$) (H$_2$PO$_4$) studied by ^{1}H solid-state NMR,[7–10] which is suitable to study the dynamics at atomic levels. We concluded that the proton transport takes place through reorientation of the tetrahedral SO$_4$ and/or PO$_4$ anions, which limits the total transport rate, and that the transfer of a proton from a tetrahedron to a neighboring one along a hydrogen bond is very rapid. We also determined correlation times of the SO$_4$/PO$_4$ reorientation and the obtained parameters well explained the macroscopic electric conductivity.

In the present work, we have studied proton dynamics in Rb$_3$H(SO$_4$)$_2$ by means of ^{1}H solid-state NMR. Rb$_3$H(SO$_4$)$_2$ is one of the hopeful inorganic solid acids in the M_3H(XO$_4$)$_2$ family.[11,12] This compound is characterized by a zero-dimensional network of hydrogen bonds, which connects two sulfate anions to form an isolated dimer, [SO$_4$-H$\cdots$SO$_4$]$^{3-}$. Thus, low-temperature phenomena such as the order-disorder mechanism and the proton tunneling have attracted much attention and have extensively been investigated by NMR,[13–17] calorimetry,[18] dielectric measurements,[19]

neutron diffraction,[20] IR,[20–22] and Raman scattering[20–22] for protonated and deuterated samples. However, proton dynamics in Rb$_3$H(SO$_4$)$_2$ has not been clarified experimentally in a high temperature range. The phase transition from the room temperature (RT) phase to the high temperature (HT) phase takes place at T_{sp}=495 K.[22]

In this work, we have measured and analyzed ^{1}H magic-angle-spinning (MAS) NMR spectra, NMR spectra for static samples (static NMR spectra) and spin-lattice relaxation times. We discuss the proton dynamics in both RT and HT phases of Rb$_3$H(SO$_4$)$_2$. The proton dynamics in Rb$_3$H(SO$_4$)$_2$ is found to be much different from those in CsHSO$_4$ and Cs$_2$(HSO$_4$)(H$_2$PO$_4$).

II. EXPERIMENT

Rb$_3$H(SO$_4$)$_2$ crystals were grown by slow evaporation of the aqueous solution containing stoichiometric amounts of Rb$_2$SO$_4$ and H$_2$SO$_4$ purchased from Junsei Chemical (Tokyo). The crystalline powder obtained was dried *in vacuo* and then sealed in glass tubes with helium gas for measurements of static NMR spectra and spin-lattice relaxation times (T_1).

The x-ray powder diffraction pattern was measured by a Rigaku MiniFlex diffractometer with Cu $K\alpha$ radiation at room temperature. The DSC measurement was performed with Rigaku ThermoPlus DSC8230 in the range of 160–570 K at heating and cooling rates of 5 K min^{-1}.

The ^{1}H MAS NMR spectra were traced at room temperature using a Bruker MSL400 spectrometer at 400.13 MHz. A Bruker MAS probehead with a 4-mm zirconia rotor was used. The ordinary single pulse sequence was used with a $\pi/4$ pulse and a recycle delay of 100 s. The frequency scale of the spectrum was expressed with respect to neat tetramethylsilane (TMS) by adjusting the signal of adamantane spinning at 8.0 kHz to 1.87 ppm.[9,10]

The measurements of ^{1}H static NMR spectra were performed with a Bruker ASX200 spectrometer at Larmor frequency of 200.13 MHz in the range of 165–513 K. They were also carried out with a Bruker ASX400 spectrometer at 400.13 MHz in 300–513 K in order to clarify the frequency dependence of the line shapes. Bruker probeheads with a solenoid coil were used. The solid echo pulse sequence ($90°_x$-τ_1-$90°_y$-τ_2-echo) was used to trace the spectra and the latter half of the echo signal was Fourier transformed. The τ_1 value was set at 8.0 μs, and the τ_2 value was the same as or slightly longer than the τ_1 value in order to acquire the signal from the echo top. The frequency scale of the spectra is expressed with respect to neat TMS by adjusting the signal of pure H_2O to 4.877 ppm.[23]

The measurement of [1]H T_1 was performed with a Bruker ASX200 spectrometer at 200.13 MHz in the range of 260–513 K. The pulse sequences used were the inversion recovery and the progressive saturation recovery followed by the solid echo pulse sequence, which were $180°$-τ-$90°_x$-τ_1-$90°_y$-τ_2-echo and $(90°$-$\tau_3)_n$-τ-$90°_x$-τ_1-$90°_y$-τ_2-echo, respectively. The values of τ_1, τ_2, and τ_3 were 8.0 μs, equal to or slightly longer than 8.0 μs and 30 μs, respectively. The T_1 values were also measured by a Bruker Minispec mq20 spectrometer at 19.65 MHz in the range of 260–470 K to clarify the frequency dependence of T_1. The inversion recovery ($180°$-τ-$90°$) and the saturation recovery ($90°$-τ-$90°$) pulse sequences were used, where τ denoted the variable delay time.

III. RESULTS AND DISCUSSION

A. X-ray powder diffraction and thermal analysis

The x-ray powder diffraction pattern observed at room temperature agrees well with literature data.[24] Thus, we confirm that the sample is RT phase of $Rb_3H(SO_4)_2$.

DSC shows an endothermic thermal anomaly at 480 K (-20.5 ± 1.2 kJ mol^{-1}) and an exothermic one at 434 K with increasing and decreasing temperature, respectively, at the first cycle of heating and cooling up to about 520 K. After the experience of the HT phase, the endothermic anomaly shows the lower temperature shift to 476 K and a small additional one appears at about 460 K in the heating processes. A melting peak is observed at 547 K (-11.6 kJ mol^{-1}).

B. ^{1}H MAS NMR spectra

Figure 1 shows a ^{1}H MAS NMR spectrum observed at room temperature (294 K). A single isotropic peak is observed at 16.3 ppm with spinning sidebands. This result demonstrates that all protons locate at a crystallographically equivalent site. In other words, all the isolated dimers are equivalent.[24] Eckert *et al.* presented the following relationship between the ^{1}H chemical shift and the hydrogen-bond strength:[25]

$$\delta_{iso}(\text{ppm}) = 79.05 - 255d(\text{O-H}\cdots\text{O})(\text{nm}) \qquad (1)$$

where $d(\text{O-H}\cdots\text{O})$ is the O-H$\cdots$O distance. The observed chemical shift suggests that the O-H$\cdots$O distance is
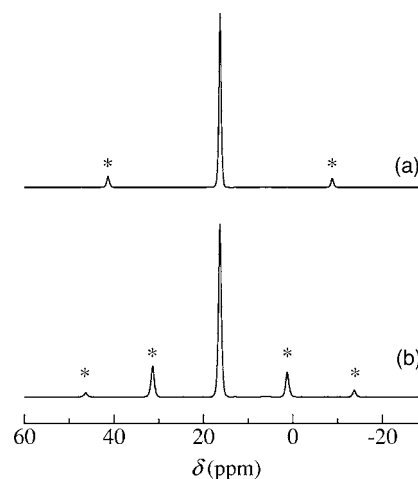
FIG. 1. ^{1}H MAS NMR spectra of $Rb_3H(SO_4)_2$, measured at 400.13 MHz and at room temperature (294 K). The spinning rates of the sample were (a) 10 and (b) 6 kHz. The recycle delay was 100 s. The marks * indicate spinning sidebands.

0.246 nm. The crystal structure study supports the above discussion; the O-H$\cdots$O distance at 292 K is 0.2485 nm. The chemical shift in this sample is larger than 12.6 and 11.2 ppm in phases III and II, respectively, of $CsHSO_4$,[9] 13.4 and 11.6 ppm in $Cs_2(HSO_4)(H_2PO_4)$ at 298 K (Ref. 10) and 14.5 and 10.9 ppm in CsH_2PO_4.[26] Thus, the hydrogen bond in $Rb_3H(SO_4)_2$ is stronger than those in the above inorganic solid acids.

C. ^{1}H static NMR spectra

Taking into account the DSC result, we perform the static NMR measurements only for the samples in the first cycle of heating from 165 K and the subsequent cooling. Figure 2 shows ^{1}H static NMR spectra measured by raising the tem-
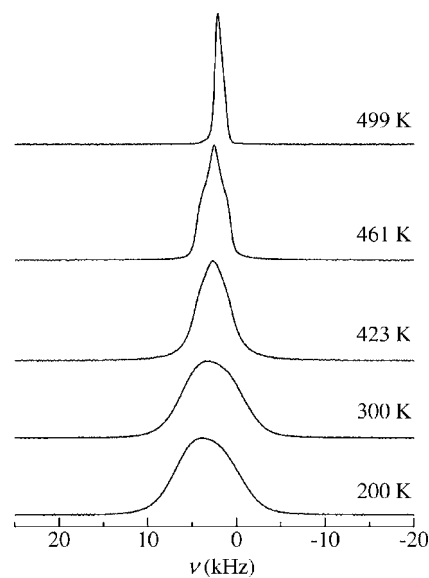
FIG. 2. ^{1}H static NMR spectra, measured at 200.13 MHz by raising the temperature from 200 to 499 K.
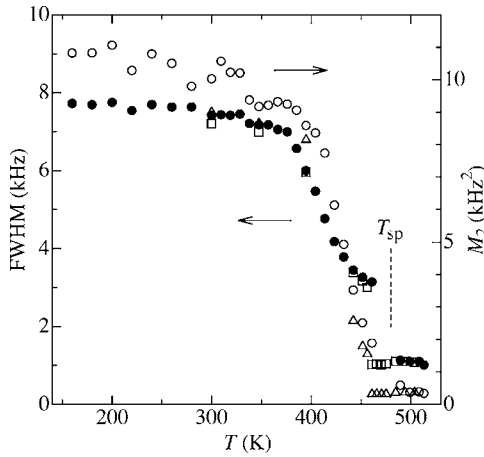
FIG. 3. Temperature dependences of the full width at half-maximum (FWHM) and the second moment (M_2) in ¹H static NMR spectra. Solid circles and open squares are FWHM measured with increasing and decreasing the temperature, respectively. Open circles and triangles indicate M_2 values on heating and cooling, respectively.

perature. These spectra show motional narrowing. Figure 3 shows temperature dependences of the linewidth and the second moment of ¹H spectra measured at 200.13 MHz. The linewidth is almost independent of temperature up to 380 K. The motional narrowing takes place from 380 K to 460 K, and then the linewidth decreases discontinuously due to the phase transition.

Protons are considered to be in an almost rigid state below 380 K. The second moment in a rigid state can be calculated from the crystal structure. In $Rb_3H(SO_4)_2$, ¹H, ⁸⁵Rb, and ⁸⁷Rb spins are taken into account, while S and O can be neglected. The ¹H linewidth has usually its origin in the dipolar interaction with ¹H, ⁸⁵Rb, and ⁸⁷Rb. The second moments for powder samples are given by[27,28]

$$M_2 = M_{HH} + M_{HRb1} + M_{HRb2}, \qquad (2)$$

$$M_{HH} = \frac{3}{5}\frac{\gamma_H^4 \hbar^2}{4\pi^2} I_H(I_H+1)\sum_i \frac{1}{r_i^6}, \qquad (3)$$

$$M_{HRb1} = 0.7215 \cdot \frac{4}{15}\frac{\gamma_H^2 \gamma_{Rb1}^2 \hbar^2}{4\pi^2} I_{Rb1}(I_{Rb1}+1)\sum_j \frac{1}{r_j^6}, \quad (4)$$

$$M_{HRb2} = 0.2785 \cdot \frac{4}{15}\frac{\gamma_H^2 \gamma_{Rb2}^2 \hbar^2}{4\pi^2} I_{Rb2}(I_{Rb2}+1)\sum_k \frac{1}{r_k^6}, \quad (5)$$

where M_{HH}, M_{HRb1}, and M_{HRb2} are the second moments due to ¹H-¹H, ¹H-⁸⁵Rb, and ¹H-⁸⁷Rb dipole-dipole interactions, respectively, in Hz units (taking into account a natural abundance of each Rb isotope), γ_H, γ_{Rb1}, and γ_{Rb2} are gyromagnetic ratios of ¹H, ⁸⁵Rb, and ⁸⁷Rb spins, respectively, $\hbar$ is Planck constant, r_i, r_j, and r_k are distances between ¹H spins, between ¹H and ⁸⁵Rb spins and between ¹H and ⁸⁷Rb spins, respectively, I_H, I_{Rb1}, and I_{Rb2} are nuclear spin quantum numbers of ¹H, ⁸⁵Rb, and ⁸⁷Rb spin, which are 1/2, 5/2, and
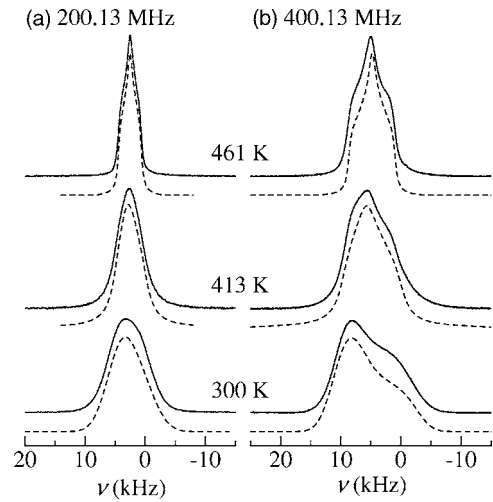
FIG. 4. ¹H static NMR spectra, measured at (a) 200.13 and (b) 400.13 MHz by raising the temperature. The dashed lines indicate the simulated line shapes.

3/2, respectively, and 0.7215 and 0.2785 are natural abundances of ⁸⁵Rb and ⁸⁷Rb, respectively.

From the crystal structure of RT phase,[24] the second moments are calculated, which are $M_{HH}=1.47$ kHz², $M_{HRb1}=0.78$ kHz², and $M_{HRb2}=1.48$ kHz². Consequently, the calculated total second moment is 3.73 kHz². The observed value of about 10 kHz² is, however, much larger than the calculated one, which indicates that ¹H spectral line shapes are not interpreted by only the dipole-dipole interactions. Chemical shift anisotropy contributes to the second moment, as is the case of $CsHSO_4$.[7] These results demonstrate that negligible proton motions take place below 380 K.

The motional narrowing starts at about 380 K. However, it stops at the linewidth of about 3 kHz. Note that the line shape at 461 K has a fine structure (Fig. 2). The fine structure suggests that chemical shift anisotropy contributes to the line shape. To conclude it, we have measured the ¹H static spectra at 400.13 MHz as well as at 200.13 MHz. ¹H static spectra observed at 400.13 MHz are broader than those at 200.13 MHz in the temperature range studied when expressed in Hz units, as shown in Fig. 4. This indicates that the line shapes are broadened by chemical shift anisotropy as well as by the dipole-dipole interactions. If expressed in Hz unit, the former is proportional to the measuring frequency, whereas the latter is independent of it.

The spectral line shapes can be fitted by a static pattern, i.e., a pattern for a rigid state. The chemical shift parameters are evaluated by simulating the spectral line shapes at the two measuring frequencies simultaneously. Three principal components of a chemical shift tensor (δ_{11}, δ_{22}, δ_{33}) are defined as $|\delta_{33}-\delta_{iso}| \geqslant |\delta_{11}-\delta_{iso}| \geqslant |\delta_{22}-\delta_{iso}|$.[27] The δ_{iso} value is an isotropic chemical shift, which is

$$\delta_{iso} = \tfrac{1}{3}(\delta_{11} + \delta_{22} + \delta_{33}). \qquad (6)$$

The η_C value is an asymmetry factor and defined as
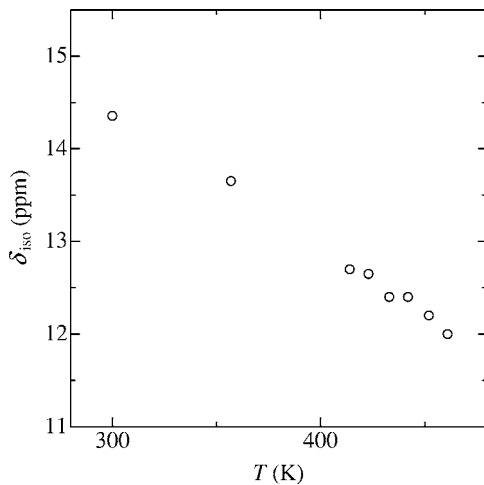
FIG. 5. Temperature dependence of δ_{iso} estimated from ^{1}H static NMR spectra.

$$\eta_C = \frac{\delta_{22} - \delta_{11}}{\delta_{33} - \delta_{iso}} \quad (0 \leq \eta_C \leq 1). \quad (7)$$

The δ_{anis} value is the magnitude of chemical shift anisotropy and is defined as

$$\delta_{anis} = \delta_{33} - \delta_{iso}. \quad (8)$$

The ^{1}H spectra at each temperature can well be explained by the chemical shift anisotropy broadened furthermore by the dipole-dipole interactions. The temperature dependence of δ_{iso} is shown in Fig. 5, while those of δ_{anis} and η_C are plotted in Fig. 6. The estimated δ_{iso} value decreases with raising the temperature, which indicates that the hydrogen bond becomes weaker gradually. The δ_{anis} value also decreases with raising the temperature, and is not averaged out even just below the transition temperature to HT phase, T_{sp}. The η_C value increases with increase in temperature and becomes close to 1 just below T_{sp}. These results indicate that the proton motion is local and anisotropic.
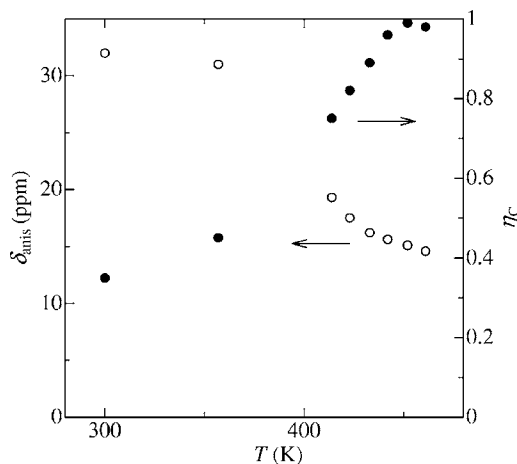
FIG. 6. Temperature dependences of δ_{anis} and η_C, estimated from ^{1}H static NMR spectra. Open and solid circles correspond to δ_{anis} and η_C, respectively.
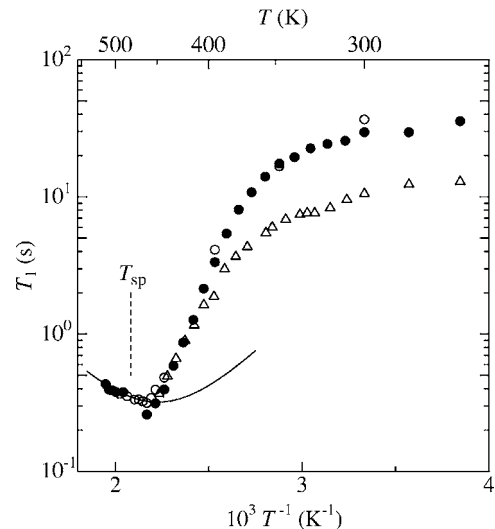
FIG. 7. Temperature and frequency dependences of ^{1}H T_1. Open triangles correspond to the results at 19.65 MHz with increasing temperature. Solid and open circles indicate the results at 200.13 MHz measured with increasing and decreasing the temperature, respectively. The solid line is the best-fitted curve in HT phase, applying Eqs. (10) and (12) in the text.

In HT phase the ^{1}H static NMR line shapes have no fine structure, as shown in Fig. 2. The linewidth and the second moment decrease discontinuously at the phase transition temperature, as shown in Fig. 3. They are almost independent of temperature above the transition temperature. The observed second moment in HT phase is about 0.3 kHz^2, which demonstrates that protons undergo translational diffusion.

D. ^{1}H spin-lattice relaxation times

The relaxation curves are single exponential at both 200.13 and 19.65 MHz. Figure 7 shows the obtained T_1 values. The T_1 values decrease gradually up to 350 K and then rapidly above 350 K with raising the temperature in RT phase. Frequency dependence is observed below 400 K, whereas it is not observed above 400 K. In HT phase, the T_1 value increases gradually with increasing temperature. The slope of the temperature dependence is slightly getting larger with increase in temperature. Unfortunately, frequency dependence in HT phase was not measured due to the instrumental limitation.

The T_1 values are discussed theoretically. The most dominant relaxation mechanism in the present system is fluctuation of dipole-dipole interaction. As described above, ^{1}H, ^{85}Rb, and ^{87}Rb spins should be taken into account in Rb$_3$H(SO$_4$)$_2$, while S and O can be neglected. Consequently, fluctuation of the dipole-dipole interactions between ^{1}H spins, between ^{1}H and ^{85}Rb spins and between ^{1}H and ^{87}Rb spins causes the ^{1}H spin-lattice relaxation. According to the theory of Bloembergen, Purcell, and Pound (BPP),[27,31] the dipolar contribution to the spin-lattice relaxation is written as

$$T_{1d}^{-1} = \frac{8\pi^2}{3}\Delta M_{HH}\left(\frac{0.5\tau_H}{1+(0.5\omega_H\tau_H)^2} + \frac{2\tau_H}{1+(\omega_H\tau_H)^2}\right)$$

$$+ 4\pi^2\Delta M_{HRb1}\left(\frac{0.5\tau_H}{1+\{(\omega_H-\omega_{Rb1})\tau_H\}^2} + \frac{1.5\tau_H}{1+(\omega_H\tau_H)^2}\right.$$

$$\left.+ \frac{3\tau_H}{1+\{(\omega_H+\omega_{Rb1})\tau_H\}^2}\right)$$

$$+ 4\pi^2\Delta M_{HRb2}\left(\frac{0.5\tau_H}{1+\{(\omega_H-\omega_{Rb2})\tau_H\}^2} + \frac{1.5\tau_H}{1+(\omega_H\tau_H)^2}\right.$$

$$\left.+ \frac{3\tau_H}{1+\{(\omega_H+\omega_{Rb2})\tau_H\}^2}\right) \quad (9)$$

where ω_H, ω_{Rb1} and ω_{Rb2} are angular resonance frequencies of ¹H and ⁸⁵Rb and ⁸⁷Rb, respectively. A mean residence time of H is denoted as τ_H. Assuming that only H is mobile, correlation times between ¹H spins and between ¹H spin and ⁸⁵Rb/⁸⁷Rb spin are $\tau_{HH}=0.5$, τ_H, and $\tau_{HRb1}=\tau_{HRb2}=\tau_H$, respectively. The values of ΔM_{HH}, ΔM_{HRb1}, and ΔM_{HRb2}, are the second moments contributing to the relaxation due to ¹H-¹H, ¹H-⁸⁵Rb, and ¹H-⁸⁷Rb dipole-dipole interactions, respectively, in Hz units.

The τ_H value is a function of temperature, and it is assumed to obey Arrhenius relation as

$$\tau_H(T) = \tau_0\exp\left(\frac{E_a}{RT}\right), \quad (10)$$

where τ_0 is a mean residence time at the infinite temperature or the inverse of a frequency factor, E_a is an activation energy and R is the gas constant.

Equations (9) and (10) predict that the plot of T_{1d} versus the inverse of temperature has a minimum, where $\omega_H\tau_H\cong 1$, and that it is symmetric with respect to the minimum position. Moreover, these equations also predict ω_H^2 dependence of T_{1d} at low temperatures where $\omega_H\tau_H\gg 1$. At high temperatures where $\omega_H\tau_H\ll 1$, the T_{1d} value is independent of ω_H, or the measuring frequency. However, significant deviation from the ω_H^2 dependence is present in RT phase, although the temperature dependence might indicate that the observed T_1 values are in the low-temperature side.

Another relaxation mechanism to be considered is fluctuation of ¹H anisotropic chemical shift. Fluctuation of anisotropic chemical shift contributes to the relaxation as follows:[27]

$$T_{1CA}^{-1} = \frac{3}{10}\omega_H^2(\Delta C_{anis})^2\frac{\tau_H}{1+\omega_H^2\tau_H^2}, \quad (11)$$

where ΔC_{anis} is the square root of the difference between the $\delta_{anis}^2(1+\eta_C^2/3)$ values at low and high temperature. Equations (10) and (11) predict that the plot of T_{1CA} versus the inverse of temperature has a minimum, where $\omega_H\tau_H\cong 1$, and that it is symmetric with respect to the minimum position, similarly to that of T_{1d}. The frequency dependence of T_{1CA}, however, differs remarkably from that of T_{1d}. The minimum value is inversely proportional to ω_H. Moreover, these equations also predict ω_H^{-2} dependence of T_{1CA} at high temperatures where $\omega_H\tau_H\ll 1$. At low temperatures where $\omega_H\tau_H\gg 1$, the T_{1CA}

value is independent of ω_H. Consequently, the contribution of this mechanism increases with the measuring frequency.

Both the dipole-dipole interaction and the anisotropic chemical shift interaction contribute to the relaxation

$$\frac{1}{T_1} = \frac{1}{T_{1d}} + \frac{1}{T_{1CA}}. \quad (12)$$

Takeda et al.[13] and Mikac et al.[17] have already reported the phonon-assisted proton tunneling at low temperatures and the thermally activated jump between the two equilibrium sites in the hydrogen bond around 300 K. On the other hand, proton dynamics has not been discussed in the temperature range above 400 K, where the T_1 value decreases rapidly without the frequency dependence. First, we attempt to analyze the T_1 values above 400 K in RT phase, using Eq. (12), in order to estimate the mean residence time of protons.

If only the dipole-dipole interactions contribute to the relaxation, the calculated T_1 minimum value is 6.9 s at 200.13 MHz, which is estimated by using the values; $\Delta M_{HH}=M_{HH}=1.47$ kHz², $\Delta M_{HRb1}=M_{HRb1}=0.78$ kHz², and $\Delta M_{HRb2}=M_{HRb2}=1.48$ kHz² obtained from the crystal structure.[24] However, the shortest T_1 value observed in RT phase (0.26 s) is much shorter than the above value. We should take into account the contribution of chemical shift anisotropy. The ΔC_{anis} value is assumed to be 28 ppm (5.6 kHz at Larmor frequency of 200.13 MHz), which is estimated from the values, $\delta_{anis}=32$ and 15 ppm and $\eta_C=0.35$ and 0.98 at 300 and 461 K, respectively. This value is comparable with the value in KH₂PO₄ ($\delta_{anis}=25$ ppm).[29] The T_1 minimum value decreases down to 2.7 s by adding the contribution of the chemical shift anisotropy. This value is, however, still larger than the observed one. A ΔC_{anis} value larger than 1000 ppm is necessary to explain the observed shortest T_1 value. This value is unreasonable, although large contribution of the chemical shift anisotropy is adequate to explain the negligible frequency dependence. We will discuss proton dynamics consistent with the above NMR results in Sec. III E.

In HT phase, the T_1 values seem to be at the slightly higher temperature side of the minimum. The second moments are calculated as $M_{HH}=14.3$ kHz², $M_{HRb1}=1.15$ kHz², and $M_{HRb2}=2.18$ kHz², by assuming the same crystal structure as the analogous phase of (NH₄)₃H(SO₄)₂.[30] The calculated T_1 minimum value is 1.2 s when $\Delta M_{HH}=M_{HH}$, $\Delta M_{HRb1}=M_{HRb1}$, $\Delta M_{HRb2}=M_{HRb2}$, and $\Delta C_{anis}=33$ ppm. This value is too long to explain the experimental one (0.3 s). We will discuss proton dynamics in HT phase in Sec. III F.

E. Proton dynamics in RT phase

In this section we will discuss proton dynamics in RT phase above 400 K. The second moment indicates that protons are in the rigid state below 380 K. The line shape of ¹H NMR spectra changes remarkably above 380 K. The line shapes are broadened by chemical shift anisotropy, demonstrating that the proton motion is local and anisotropic. The obtained chemical shift parameters shown in Fig. 6 suggest that the possible proton motion is two-site jump or its ana-

(a)

(b)
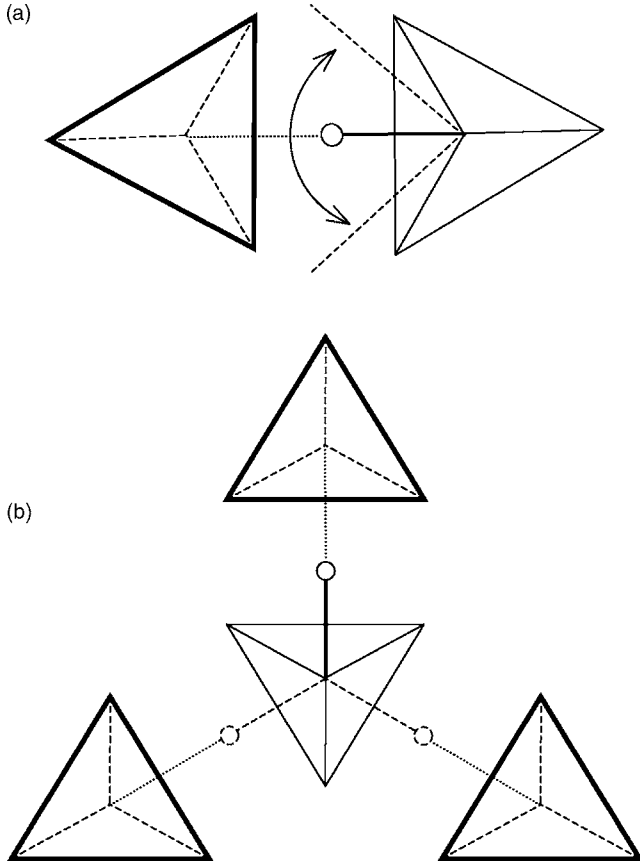
FIG. 8. Schematic pictures of proton dynamics: (a) The wobbling motion of the O-H bond in one direction in RT phase, and (b) the dynamical two-dimensional hydrogen bond network inducing proton diffusion in HT phase. Tetrahedra and spheres show SO_4 anions and protons, respectively.

logue. In the same temperature range, the T_1 value decreases rapidly with temperature. In principle, the line shape is sensitive to the motion of the order of the linewidth (10 kHz), whereas T_1 is sensitive to the motion of the order of the measuring frequency (20 and 200 MHz). In the present case, however, the same motion contributes to the change of the line shape and the relaxation. Furthermore, no frequency dependence of T_1 is observed above 400 K in RT phase, though the T_1 value seems to locate at the low temperature side of the minimum. The frequency independence indicates that the proton motion is in the fast motional limit. Taking all the above results into consideration, the most probable motion is a wobbling motion in one direction shown in Fig. 8(a) schematically. The rate of the motion is in the fast motional limit and its amplitude increases as the temperature increases. The increase of the wobbling amplitude causes the changes of both the line shape and T_1. The δ_{iso} value decreases with increasing the temperature, as shown in Fig. 5, indicating that hydrogen bonds become weak due to the wobbling motion.

The line shape change due to the wobbling motion is described theoretically based on the theory for quadrupolarly perturbed lines.[31,32] We consider two-site jump first, and then wobbling in one direction.

(1) Two-site jump, $\theta = +\theta_1$ and $-\theta_1$,

$$\delta_{11} - \delta_{iso} = -\frac{\delta_{anis,0}}{2}(1 + \eta_0), \tag{13}$$

$$\delta_{22} - \delta_{iso} = +\frac{\delta_{anis,0}}{4}[(1 - 3\cos 2\theta_1) + \eta_0(1 + \cos 2\theta_1)], \tag{14}$$

$$\delta_{33} - \delta_{iso} = +\frac{\delta_{anis,0}}{4}[(1 + 3\cos 2\theta_1) + \eta_0(1 - \cos 2\theta_1)], \tag{15}$$

and $\delta_{12} = \delta_{23} = \delta_{13} = \delta_{iso}$, where $\delta_{anis,0}$ and η_0 are the magnitude of chemical shift anisotropy and an asymmetry factor both in a rigid state, respectively. For $0 \leq \theta_1 \leq \theta_m(\cos 2\theta_m = 1/3)$:

$$\delta_{anis} = \delta_{anis,0}\frac{1 + 3\cos 2\theta_1}{4}, \tag{16}$$

$$\eta_C = \frac{3(1 - \cos 2\theta_1)}{1 + 3\cos 2\theta_1} \tag{17}$$

(2) Wobbling in one direction, θ is varied between $+\theta_1$ and $-\theta_1$ continuously. The population is assumed to be constant for simplicity. Integration from $\theta = +\theta_1$ and $-\theta_1$ is performed.

(2-1) For $0 \leq \theta_1 \leq \theta_{m1}(\sin 2\theta_{m1}/2\theta_{m1} = (1 - \eta_0)/(3 - \eta_0))$,

$$\delta_{anis} = \delta_{anis,0}\frac{1 + 3\sin 2\theta_1/2\theta_1 + \eta_0(1 - \sin 2\theta_1/2\theta_1)}{4}, \tag{18}$$

$$\eta_C = \frac{3(1 - \sin 2\theta_1/2\theta_1) + \eta_0(3 + \sin 2\theta_1/2\theta_1)}{1 + 3\sin 2\theta_1/\theta_1 + \eta_0(1 - \sin 2\theta_1/2\theta_1)}. \tag{19}$$

(2-2) For $\theta_{m1} \leq \theta_1 \leq \pi$,

$$\delta_{anis} = \tfrac{1}{2}\delta_{anis,0}(1 + \eta_0), \tag{20}$$

$$\eta_C = \frac{(3 - \eta_0)\sin 2\theta_1}{2\theta_1(1 + \eta_0)}. \tag{21}$$

(2-3) For $\pi \leq \theta_1 \leq 2\pi$,

$$\delta_{anis} = \tfrac{1}{2}\delta_{anis,0}(1 + \eta_0), \tag{22}$$

$$\eta_C = \frac{(\eta_0 - 3)\sin 2\theta_1}{2\theta_1(1 + \eta_0)}. \tag{23}$$

By using Eqs. (19) and (21), the range of wobbling angles $2\theta_1$ are estimated, where η_0 is assumed to be 0.35 from the experimental value at 300 K. The wobbling angle $2\theta_1$ is getting larger up to about 110° just below T_{sp}. Next, we have checked whether Eqs. (18) and (20) hold or not. The chemical shift anisotropy in a rigid state $\delta_{anis,0}$ can be estimated by using the $2\theta_1$ value and Eqs. (18) and (20). The estimated $\delta_{anis,0}$ value decreases above 400 K, as shown in Fig. 9, which suggests that the hydrogen bond becomes weaker.
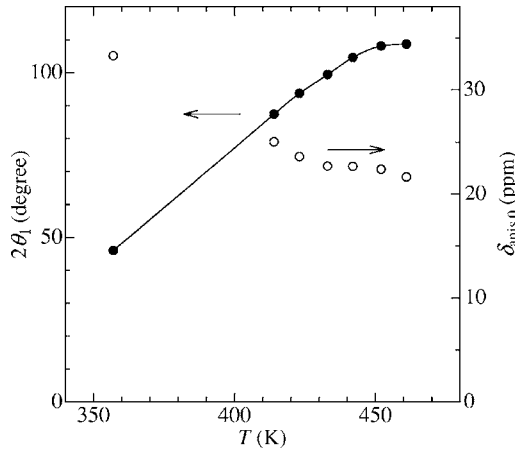
FIG. 9. Temperature dependences of the wobbling angle $2\theta_1$ and the chemical shift anisotropy in a rigid state $\delta_{\text{anis},0}$. The $2\theta_1$ value is calculated by using Eqs. (19) and (21) with $\eta_0=0.35$. The $\delta_{\text{anis},0}$ is calculated by using Eqs. (18) and (20) with $\eta_0=0.35$ and the above $2\theta_1$ value. The solid curve is a guide to the eye.

Weakening of the hydrogen bond is also demonstrated by the change of the isotropic chemical shift. Thus, the proposed motion can explain the temperature dependence of the ¹H static spectra, although the parameters shown in Fig. 9 are obtained from very rough estimation.

The reason of the very short T_1 values above 400 K in RT phase is discussed below, relating to the wobbling motion: In RT phase, the distance between the nearest H atoms is considered not to vary so much because each H atom locates on a site in the isolated dimer. On the other hand, the distance between H and Rb atoms can be shorter due to the wobbling motion of the O-H bond. The shortest T_1 value in RT phase can be reproduced by using $\Delta M_{\text{HH}}=1.47$ kHz² calculated from the crystal structure and $\Delta C_{\text{anis}}=28$ ppm and by assuming $\Delta M_{\text{HRb1}}=18$ kHz² and $\Delta M_{\text{HRb2}}=35$ kHz², which are much larger than those estimated from the crystal structure. The shortest O-Rb distance is about 0.31 nm, being calculated from the crystal structure. The instantaneous minimum distance between H and Rb is required to be about 0.152 nm if a ¹H-Rb spin pair is assumed to be isolated from the other spins. The required minimum distance between H and Rb might become a little bit longer by considering the effect of other surrounding spins. The ¹H spin is surrounded by four Rb ions. The short instantaneous minimum H-Rb distance may be realized by the wobbling motion as well as the rocking motion of the HSO₄ ions and the lattice vibration of Rb ions. If the O-H bond directs to a Rb ion, the $2\theta_1$ value agrees with $\angle$Rb⋯O⋯Rb (134° from the crystal structure in RT phase). As described above, the $2\theta_1$ value increases with temperature up to about 110°. The isolated dimer, [SO₄-H⋯SO₄]³⁻ is considered to have large flexibility in its orientation, because it is not connected with surrounding ions covalently, although the hydrogen bond in the dimer restricts the orientation of the two SO₄ tetrahedra. This might indicate that the potential energy curve for the orientaion of the dimer is rather flat. No translational proton diffusion takes place in RT phase.

F. Proton dynamics in HT phase

The observed ¹H signal in HT phase is very sharp and its second moment is negligibly small, indicating that protons undergo translational diffusion. Thus, we attempt to analyze the T_1 results to estimate the proton diffusion rate.

First, we should discuss the reason for the much shorter T_1 values in HT phase than the calculated value. The distance between the nearest H atoms is considered not to vary so much, whereas the distance between H and Rb atoms can be shorter in the midway of the translational movement of H. By assuming the crystal structure of analogous $(NH_4)_3H(SO_4)_2$, $\Delta M_{\text{HH}}=M_{\text{HH}}=14.3$ kHz². The contribution of chemical shift anisotropy is assumed as $\Delta C_{\text{anis}}=33$ ppm. The T_1 minimum value in HT phase can be reproduced by assuming $\Delta M_{\text{HRb1}}=12$ kHz² and $\Delta M_{\text{HRb2}}=23$ kHz², which correspond to the instantaneous minimum distance between H and Rb of about 0.163 nm if a ¹H-Rb spin pair is assumed to be isolated from the other spins. The minimum distance between H and Rb is about 0.17 nm at the midway of proton jump between stable sites, being estimated from the crystal structure of analogous $(NH_4)_3H(SO_4)_2$.Then, the above magnitudes of dipolar fluctuations are considered to be reasonable if taking into account the lattice vibration of Rb ions additionally. The temperature dependence of ¹H T_1 in HT phase is fitted by Eq. (12), as shown in Fig. 7. The obtained parameters are $E_a=25$ kJ mol⁻¹ and $\tau_0=9.5\times10^{-13}$ s. Because the temperature range in HT phase is very narrow, the fitting might contain considerable errors. However, the presence of the further small T_1 minimum value is unrealistic, because the still larger dipole-dipole interactions between ¹H and ^{85}Rb/^{87}Rb should work.

Diffusion constants are related to the mean residence time of protons by the following equation:[7,8,10]

$$D = \frac{L^2}{n\tau_{\text{H}}}, \tag{24}$$

where L is a jumping distance and n is the number of sites to which H can jump. As the sample studied here is in a powder form, the macroscopic D value is an average of all spatial directions. The n value is assumed to be 6 in order to compare with the electric conductivity data in a powder sample, though the value is considered to be 4 in two-dimensional diffusion predicted by the crystal structure. The D value obeys the Arrhenius relation as

$$D = D_0 \exp\left(-\frac{E_a}{RT}\right), \tag{25}$$

where D_0 is a constant independent of temperature.

A jump between the sites on the SO₄ tetrahedra is a unit step of the translational diffusion and, therefore, the mean jump length is assumed to be the interatomic distance between the nearest S atoms projected to the ab plane where the two-dimensional hydrogen bond network is formed. Consequently, the L value is estimated as 0.30 nm, by the analogy with the similar phase of $(NH_4)_3H(SO_4)_2$.[30] Thus, $E_a=25$ kJ mol⁻¹ and $D_0=1.5\times10^{-8}$ m² s⁻¹ in HT phase, using the τ_{H} value. The D value ranges from 2.2×10^{-11} to 5.8×10^{-11} m² s⁻¹ in the temperature range of 460 to 540 K.
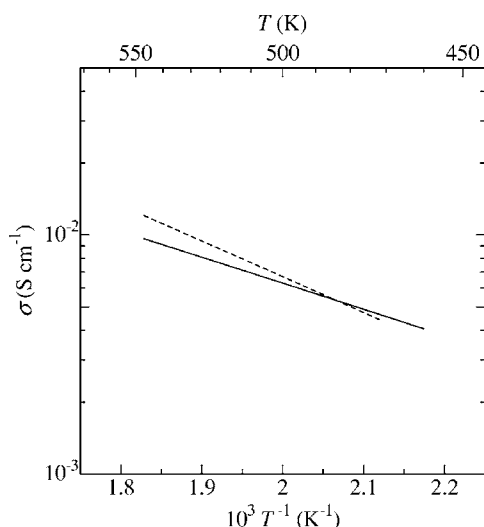
FIG. 10. Temperature dependence of proton conductivity in HT phase. The solid and the dashed lines correspond to proton conductivity data estimated from the ^{1}H NMR results and measured by the AC impedance method (Ref. 12), respectively.

The electric conductivity is related to the proton diffusion constant by the following equation:

$$\sigma = Ne^2 D/kT, \qquad (26)$$

where N is the density of mobile protons, e is the proton charge, and k is Boltzmann constant. The N value is assumed to be 4.5×10^{27} m^{-3} from the proposed crystal structure of RT phase[24] because it is known that the N values are almost the same in the RT and HT phases of $(NH_4)_3H(SO_4)_2$.[30] The estimated conductivity in the HT phase is shown in Fig. 10, which agrees well with the electric conductivity data reported by Sinitsyn.[12] The activation energy in the present work (25 kJ mol^{-1}) agrees approximately with that of the conductivity (0.34 eV=32.9 kJ mol^{-1}).[12] This confirms that the microscopic proton motion determines the macroscopic conductivity, as are the cases for CsHSO$_4$ (Refs. 7 and 8) and Cs$_2$(HSO$_4$)(H$_2$PO$_4$).[10]

The proton transport in Rb$_3$H(SO$_4$)$_2$ is thought to take place through two elementary steps;rotation of the O-H bond around the S-O axis shown in Fig. 8(b) and transfer of a proton from a tetrahedron to a neighboring one along a hydrogen bond. The above discussions are based on the mechanism that the former is much slower than the latter. The similar mechanism has been confirmed in CsHSO$_4$ (Refs. 7 and 8) and Cs$_2$(HSO$_4$)(H$_2$PO$_4$).[10] If the rotation of the O-H bond is assumed to be much faster than the proton transfer along a hydrogen bond, the proton diffusion rate should be determined by the latter proton transfer rate. In this case, the

rotation of the O-H bond averages out a part of the dipolar interactions at the lower temperatures, and only the residual dipolar interactions contribute to the relaxation in the temperature range studied. The second moments corresponding to the residual dipolar interactions are M_{HH}=0.89 kHz^2, M_{HRb1}=0.87 kHz^2, and M_{HRb2}=1.65 kHz^2, being calculated by locating every proton at the position of the oxygen atom bonding with H with the occupancy of 0.5. The estimated T_1 minimum value is 4.9 s at 200.13 MHz. It reduces to 2.4 s if the full chemical shift anisotropy (ΔC_{anis}=33 ppm) contributes to the relaxation. These values are significantly longer than the experimental one. Furthermore, the enlargement of the dipole-dipole interaction between ^{1}H and Rb is not expected to work because the rotation of the O-H bond averages out the effect. Conclusively, the rate-determining step is the rotation of the O-H bond. The proton transfer along a hydrogen bond takes place simultaneously or successively each time when the O-H bond rotates, leading to the proton translational diffusion.

The activation energy E_a of the proton conductivity in HT phase is smaller in Rb$_3$H(SO$_4$)$_2$ (25 kJ mol^{-1}) than in CsHSO$_4$ (35 kJ mol^{-1}) (Ref. 8) and Cs$_2$(HSO$_4$)(H$_2$PO$_4$) (36 kJ mol^{-1}).[10] Each XO_4 tetrahedron has only one hydrogen bond in $M_3H(XO_4)_2$, while SO$_4$ and PO$_4$ anions forms more than one hydrogen bond per tetrahedron in CsHSO$_4$ and Cs$_2$(HSO$_4$)(H$_2$PO$_4$). In all the compounds, the proton diffusion is limited by the motions breaking the hydrogen bonds. Consequently, the activation energy of the proton diffusion is affected by the number of hydrogen bonds.

IV. CONCLUSIONS

Proton dynamics in Rb$_3$H(SO$_4$)$_2$ has been studied by means of ^{1}H solid-state NMR, and the following conclusions have been obtained:

(1) The ^{1}H MAS NMR spectrum at room temperature (294 K) has an isotropic chemical shift of 16.3 ppm from TMS. This value indicates the presence of strong hydrogen bonds.

(2) In RT phase, a very fast local motion of protons takes place above 400 K, being supported by the ^{1}H static NMR spectral line shapes and by the ^{1}H T_1 values. The most probable motion is a wobbling motion of the O-H bond in one direction at the fast motional limit.

(3) In HT phase, the ^{1}H static NMR spectra demonstrate that translational proton diffusion takes place. Protons diffuse with the inverse of the frequency factor (τ_0) of 9.5 $\times 10^{-13}$ s and an activation energy (E_a) of 25 kJ mol^{-1}, being obtained from the analysis of the ^{1}H T_1 results. These parameters can well explain the macroscopic electric conductivity in this phase.

*Corresponding author. Electronic address: hayashi.s@aist.go.jp

[1] S. M. Haile, D. A. Boysen, C. R. I. Chisholm, and R. B. Merle, Nature (London) **410**, 910 (2001).

[2] D. A. Boysen, T. Uda, C. R. I. Chisholm, and S. M. Haile, Science **303**, 68 (2004).

[3] A. I. Baranov, L. A. Shuvalov, and N. M. Shchagina, JETP Lett. **36**, 459 (1982).

[4] A. Pawlowski, Cz. Pawlaczyk, and B. Hilzcer, Solid State Ionics **44**, 17 (1990).

[5] T. Norby, M. Friesel, and B. E. Mellander, Solid State Ionics **77**, 105 (1995).

[6] V. V. Sinitsyn, A. I. Baranov, E. G. Ponyatovsky, and L. A. Shuvalov, Solid State Ionics **77**, 118 (1995).

[7] M. Mizuno and S. Hayashi, Solid State Ionics **167**, 317 (2004).

[8] S. Hayashi and M. Mizuno, Solid State Ionics **171**, 289 (2004).

[9] S. Hayashi and M. Mizuno, Solid State Commun. **132**, 443 (2004).

[10] S. Hayashi and M. Mizuno, Solid State Ionics **176**, 745 (2005).

[11] Ph. Colomban and A. Novak, J. Mol. Struct. **177**, 277 (1988).

[12] V. V. Sinitsyn, A. I. Baranov, and E. G. Ponyatovsky, Solid State Ionics **136-137**, 167 (2000).

[13] S. Takeda, F. Kondoh, N. Nakamura, and K. Yamaguchi, Physica B **226**, 157 (1996).

[14] J. Dolinsek, U. Mikac, J. E. Javorsek, G. Lahajnar, R. Blinc, and L. F. Kirpichnikova, Phys. Rev. B **58**, 8445 (1998).

[15] U. Mikac, D. Arcon, B. Zalar, J. Dolinsek, and R. Blinc, Phys. Rev. B **59**, 11293 (1999).

[16] A. Titze, A. Maiazza, G. Hinze, and R. Böhmer, Phys. Rev. B **59**, 11720 (1999).

[17] U. Mikac, B. Zalar, J. Dolinsek, J. Seliger, V. Zagar, O. Plyushch, and R. Blinc, Phys. Rev. B **61**, 197 (2000).

[18] T. Matsuo, N. Tanaka, M. Fukai, O. Yamamuro, A. Inaba, and M. Ichikawa, Thermochim. Acta **403**, 137 (2003).

[19] K. Gesi, J. Phys. Soc. Jpn. **48**, 886 (1980).

[20] F. Fillaux, A. Lautié, J. Tomkinson, and G. J. Kearley, Chem. Phys. **154**, 135 (1991).

[21] N. Fourati, M. Kamoun, and A. Daoud, Phase Transitions **18**, 87 (1989).

[22] M. Polomska, L. F. Kirpichnikova, T. Pawlowski, and B. Hilczer, Ferroelectrics **290**, 51 (2003).

[23] T. Ueda, S. Hayashi, and K. Hayamizu, Solid State Commun. **87**, 429 (1993).

[24] S. Fortier, M. E. Fraser, and R. D. Heyding, Acta Crystallogr., Sect. C: Cryst. Struct. Commun. **C41**, 1139 (1985).

[25] H. Eckert, J. P. Yesinowski, L. A. Silver, and E. M. Stolper, J. Phys. Chem. **92**, 2055 (1988).

[26] D. A. Boysen, S. H. Haile, H. Liu, and R. A. Secco, Chem. Mater. **15**, 727 (2003).

[27] A. Abragam, *The Principles of Nuclear Magnetism* (Oxford University Press, Oxford, 1961).

[28] J. H. Van Vleck, Phys. Rev. **74**, 1168 (1948).

[29] J. T. Rasmussen, M. Hohwy, H. J. Jakobsen, and N. C. Nielsen, Chem. Phys. Lett. **314**, 239 (1999).

[30] K. Friese, M. I. Aroyo, L. Schwalowsky, G. Adiwidjaja, and U. Bismayer, J. Solid State Chem. **165**, 136 (2002).

[31] R. G. Barnes, Adv. Nucl. Quadrupole Reson. **1**, 335 (1974).

[32] S. Hayashi, Clays Clay Miner. **45**, 724 (1997).